PHYSICAL REVIEW B VOLUME 23, NUMBER 10 15 MAY 1981

Reflectance spectra of some $FePS_3$-type layer compounds in the vacuum ultraviolet

F. S. Khumalo* and H. P. Hughes
Physics and Chemistry of Solids, Cavendish Laboratory, Madingley Road, Cambridge CB3 0HE, England
(Received 17 March 1980; revised manuscript received 29 December 1980)

Near-normal-incidence reflectivity spectra of single crystals of $MnPS_3$, $FePS_3$, and $NiPS_3$ have been obtained in the vacuum ultraviolet region of the optical spectrum. The spectra are interpreted using molecular-orbital ideas as well as simple physical and chemical arguments. The metal *d* orbitals in these materials are envisaged as localized discrete levels (rather than bands) in the energy-band models proposed. The most illuminating result of this work is that the reflectivity features on the three spectra look identical. These similarities in the three spectra have led us to suggest that, in a broad view, the band structures (as yet unknown) of the first-row transition-metal chalcogenophosphates (archetype $FePS_3$) are closely similar. Furthermore, we conclude that for photon energies greater than the absorption edge, the localized transition-metal *d* orbitals do not seem to take part in the optical transitions (only the energy bands of the P_2S_6 complex take part), thus causing the observed similarities in the reflectivity spectra of MPS_3 systems.

I. INTRODUCTION

Transition-metal phosphorus trichalcogenides (otherwise known as transition-metal chalcogenophosphates) are layer compounds with the general chemical formula MPX_3 [where M is a first-row transition metal (with an incomplete d shell) such as Mn, Fe, and Ni; P is phosphorus and X is either S or Se]. These compounds generally crystallize as thin platelet crystals.

Magnetic-susceptibility measurements on ground polycrystalline samples of $MnPS_3$, $FePS_3$, and $NiPS_3$ indicate that these crystals are antiferromagnetic with Néel temperatures of 110°, 126°, and 253°; their Weiss constants are −263, +14, and −588 K and their magnetic moments determined in the paramagnetic region are 6.20, 5.43, and 3.68μ_B, respectively.[1-3] These moments were interpreted as indicating the presence of significant spin-orbit coupling.[2] Brec *et al.*[4] have made dc electrical-conductivity measurements, perpendicular to the c axis, on $MnPS_3$, $FePS_3$, and $NiPS_3$, among other crystals. Crystals of $NiPS_3$ were found to have extremely high resistances (~10^9 Ω cm) whereas those of $FePS_3$ and $MnPS_3$ had values between 10^4 and 10^5 Ω cm. Optical-absorption measurements on single crystals of $MnPS_3$, $FePS_3$, and $NiPS_3$ have been reported in the literature and the results indicate that members in the $FePS_3$-type family are broad-band semiconductors, with gap values of 3.0, 1.5, and 1.6 eV for $MnPS_3$, $FePS_3$, and $NiPS_3$, respectively.[4] Intense d-d transitions (which occur at energies close to the fundamental absorption edge) have been observed in these materials.[4,5]

Transition-metal dichalcogenides, such as TiS_2, have been reported in the literature to perform well as cathodes in ambient-temperature lithium batteries.[6,7] The critical feature in TiS_2 is its lamellar structure which allows the intercalation by lithium ions (and other species) between alternate sulfur layers without bond breaking. Recently, there has been a burgeoning interest in the layered transition-metal phosphorus trichalcogenides, (especially $NiPS_3$) because these compounds readily react with alkali metals and exhibit tremendous electrochemical activity. These MPX_3 systems have crystal structures very similar to that of TiS_2 (see Fig. 2). The Ni atoms and P–P pairs (in $NiPS_3$, for example) occupy the sites that titanium would fill in TiS_2. Alternate layers of interstices between the sulfur planes are unoccupied, permitting occupation by other atoms or molecules.[4,6,7] On an equivalent structural basis, MPX_3 compounds accept approximately 3 times as much lithium as does TiS_2 and furthermore, the greater capacity for lithium atoms exhibited by $NiPS_3$ leads to a theoretical density of 1 kW h/kg,[6] double that of 480 W h/kg for TiS_2.[7] If this high theoretical energy density is truly electrochemically reversible, then the low cost of the component elements, the reasonable conductivity of the iron and nickel compounds, and the ambient-temperature operation will make the Li-MPS_3 batteries promising candidates for electric-vehicle propulsion in the future.

A thorough literature survey has revealed that neither a systematic optical study nor a decent electronic band model for the $FePS_3$-type layer compounds is reported. An electronic band-structure model for these $FePS_3$-type layer compounds is needed for both academic and technological reasons; the academic interest being the high anisotropy exhibited by such compounds and their ability to intercalate foreign atoms without any parameter expansion.[4] Up to now, no attempt has

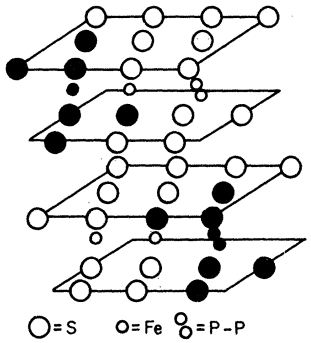

FIG. 1. Structure of $FePS_3$. The octahedral coordination about the Fe^{2+} ions and P-P pairs is shown by the darkened circles (Ref. 1).

been made to determine the electronic band structure of these $FePS_3$ systems. The vacuum ultraviolet reflectivity spectra of $MnPS_3$, $FePS_3$, and $NiPS_3$ presented in this paper and their interpretation constitutes the first-ever attempt towards the determination of the electronic energy-band scheme of these MPX_3 systems.

II. CRYSTAL STRUCTURE

The crystal structure of $FePS_3$ (as an archetype of these MPX_3 compounds) has been studied and reported by several workers.[1-13] Klingen *et al.*[10-12] performed repeated crystal-structure determinations of $FePS_3$ and found it to have a monoclinic unit cell (space group $C2/m$) with the lattice parameters $a_0 = 5.934$ Å, $b_0 = 10.28$ Å, $c = 6.722$ Å, and $\beta = 107.16°$. The structure is related to that of cadmium chloride ($CdCl_2$) with iron (FeII) ions and phosphorus-phosphorus pairs (P_2) occupying the cadmium positions and sulfur atoms occupying the chloride positions. In this way the iron (Fe) ions and P–P pairs are approximately octahedrally coordinated in a distorted cubic-closed lattice. This atomic arrangement results in FeS_6 and P_2S_6 octahedral groups. The P–P bond direction is collinear with the octahedral threefold axis and is parallel with the hexagonal c axis. The structure of $FePS_3$ is shown in Figs. 1 and 2. In Fig. 1 the octahedral coordination about the Fe^{2+} ions and P–P pairs is shown by darkened circles. Figure 3

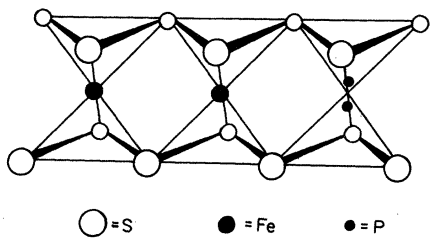

FIG. 2. Structure of $FePS_3$ showing the close structural coordination about the Ti^{2+}.

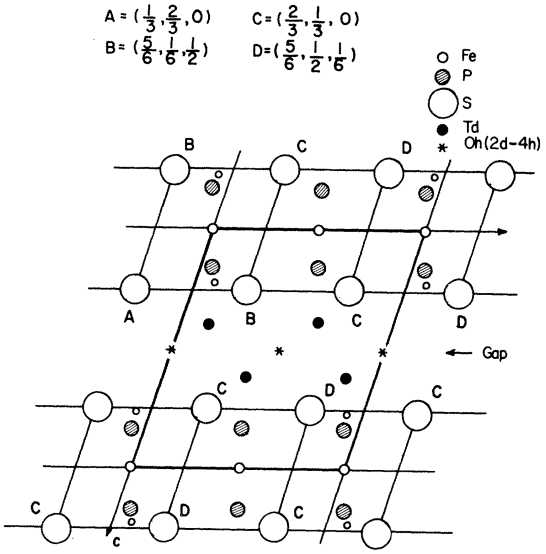

FIG. 3. Schematic diagram of the structure of MPS_3 (C_2/m) showing gaps where intercalation can occur (Ref. 4).

shows, schematically, the structure of $FePS_3$ with gaps where intercalation occurs. Figure 4 shows P_2 pairs and sulfur polyhedra of an MPS_3 compound.

III. EXPERIMENTAL DETAILS

The vacuum ultraviolet (vuv) reflectometer and the photon-counting system (with a gating system interfaced with a floppy-disc minicomputer) used to obtain the reflectivity spectra of these $MPSe_3$-type compounds have been described elsewhere.[14] The reflectivity spectra presented in this paper were obtained from the basal plane of the crystal, perpendicular to the c axis. In other words, if our vuv light were polarized, the near-normal incidence reflectivity spectra would be for $\vec{E} \perp \hat{c}$. The spectra are within ~5% of being absolute. All the spectra were repeated several times (at both room and liquid-nitrogen temperatures) to check for re-

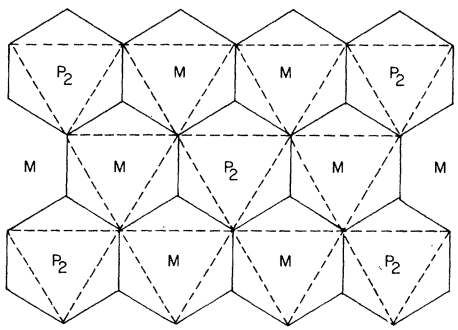

FIG. 4. Metal (M) and phosphorous pairs (P_2) in sulfur polyhedra of MPS_3 compound.

producibility. The single crystals of $MnPS_3$, $FePS_3$, and $NiPS_3$ used in this work were gratefully borrowed from Miss Lawrence Coic.[5] The general technique of preparation of single crystals (from appropriate ratios of constituent elements) was the widely used chemical vapor transport method. Crystals of $FePS_3$ and $NiPS_3$ appear as blackish metallic, flexible hexagonal plates whereas the $MnPS_3$ crystals appear as transparent green, hexagonal plates.

All samples were freshly cleaved in air using adhesive tape immediately before an experimental run, and then quickly inserted into the specimen chamber which would then be rapidly evacuated to $\sim 1\times10^{-7}$ Torr to minimize atmospheric surface contamination. A better vacuum (which was necessary for liquid-nitrogen runs) inside the specimen chamber could be obtained by use of a liquid-nitrogen tank and a radiation shield which acted as an excellent cold trap for contaminants. The data-acquisition system included a gated photon counter interfaced to a minicomputer which analyzed the data as the experiment progressed. The data were then stored in the floppy-disk system of the computer.

IV. RESULTS, BAND MODEL AND DISCUSSION

A. Results

Figures 5–7 show the near-normal incidence reflectivity spectra, at 260 and 85 K, between 3.7 and 14 eV of freshly cleaved layer faces of single crystals of $MnPS_3$, $FePS_3$, and $NiPS_3$, respectively. The reproducible reflectivity features (in eV) on the spectra are indicated by vertical short lines on the spectra. Table I shows the corresponding features (in eV) on the same line, for the three spectra at 260 and 85 K. When the three spectra were superposed, we observed the following: (i) The reflectivity features on the spectra of $MnPS_3$ and $FePS_3$ are almost identical, with the features on the $FePS_3$ spectrum shifted by a few eV to higher energies relative to those on the $MnPS_3$. (ii) The three spectra exhibit broad similarities (see Fig. 8) in their reflectivity features.

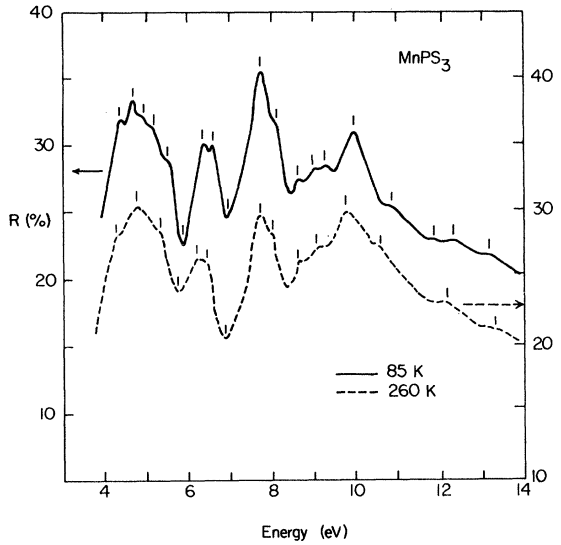

FIG. 5. vuv reflectivity spectrum of $MnPS_3$, with light incident normal to the layer plane, at 260 K (---) and 85 K (——).

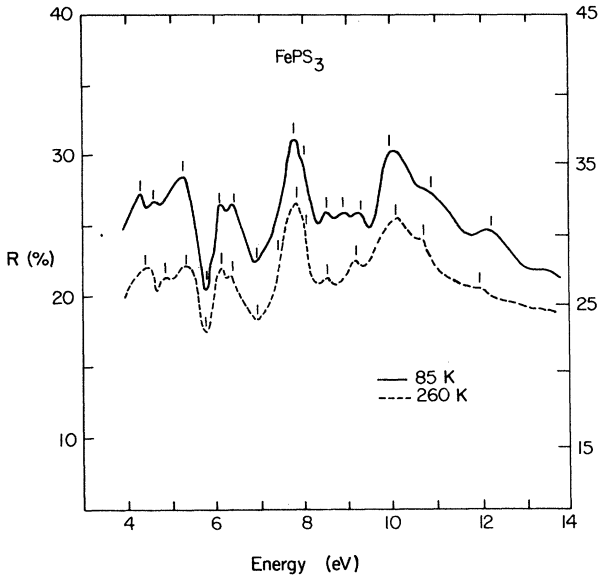

FIG. 6. vuv reflectivity spectrum of $FePS_3$, with light incident normal to the layer plane, at 260 K (---) and 85 K (——).

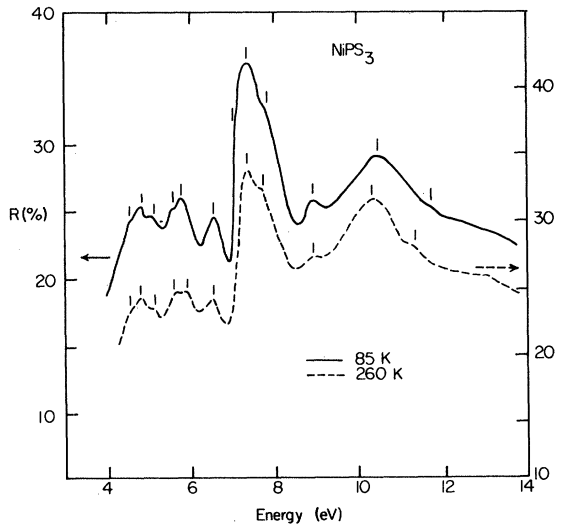

FIG. 7. vuv reflectivity spectrum of $NiPS_3$, with light incident normal to the layer plane, at 260 K (---) and 85 K (——).

TABLE I. Features (in eV) on the reflectivity spectra of $MnPS_3$, $FePS_3$, and $NiPS_3$. Corresponding structure values are shown on the same line. Asterisks indicate where prominent peaks on each spectrum occur.

$MnPS_3$		$FePS_3$		$NiPS_3$	
260 K	85 K	260 K	85 K	260 K	85 K
13.21	13.19			13.03	
12.02	12.42	11.98	12.10		
10.52	10.89	11.12	11.15	11.22	11.72
		10.01*	10.23	10.45*	10.48*
9.75*	9.86*	9.72	9.85	9.55	
9.04	9.31				
	9.00		8.96	8.95	8.95
	8.66	8.50	8.70		
	8.10				
7.46	7.49*	7.79*	7.96*	7.76	7.82
		7.62	7.72		
				7.36*	7.39
					7.24
6.92	6.93	6.85	6.92	6.90	6.87
6.42	6.56	6.36	6.37		6.33
6.25	6.38			6.17	6.15
5.78	5.86	5.75	5.78	5.84	5.75
5.29	5.51	5.44	5.51	5.26	5.29
5.06	5.20			5.01	5.09
4.78	4.90	4.74	4.83	4.78	4.79
4.54	4.68				
	4.39				
4.12	4.20				

(iii) Between ~4 and 7 eV, the spectra of $MnPS_3$ and $FePS_3$ exhibit much sharper features than the spectrum of $NiPS_3$. (iv) On all three spectra, there are two prominent peaks—at 7.5 and 10 eV for the $MnPS_3$ spectrum, at 7.8 and 10.1 eV for the $FePS_3$ spectrum, and at 7.3 and 10.5 eV for the $NiPS_3$ spectrum. (v) On cooling all the samples to 85 K, both peaks on each spectrum sharpen, with the peak at ~7 eV (especially for $NiPS_3$) sharpening considerably more than the peak at ~10 eV. Furthermore, we also observe that the peak at ~7 eV, for $NiPS_3$, completely dominates, in height, all other reflectivity features on the same spectrum or the other two spectra.

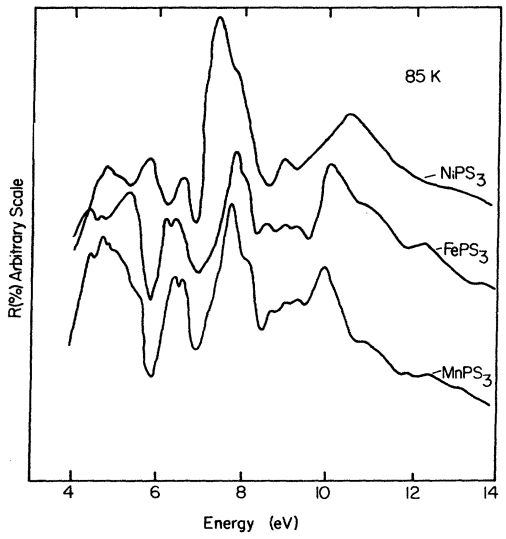

FIG. 8. Comparison of the reflectivity spectra of $MnPS_3$, $FePS_3$, and $NiPS_3$ at 85 K.

B. Energy-level model for an MPS_3 layer compound

Before discussing in detail the vacuum ultraviolet spectra of $MnPS_3$, $FePS_3$, and $NiPS_3$ shown in Figs. 5, 6, and 7, respectively, it is important to explain how we obtained the proposed energy-level models for $MnPS_3$, $FePS_3$, and $NiPS_3$ shown in Figs. 10, 11, and 12, respectively.

Crystal-structure studies[8-10] on these MPX_3 (where M = Mn, Fe, Ni and X = S or Se) compounds reveal that the atomic arrangement in these MPX_3 systems results in MX_6 and P_2X_6 octahedral groups and also that the P–P bond is (a) a very short bond[3] of distance 2.2 Å [hence the existence of bonding and antibonding P_2 (pairs) states in these compounds], (b) is collinear with the octahedral threefold axis, and (c) is parallel to the hexagonal c axis. Magnetic[1,2] and NMR[3] measurements have, too, revealed that MPX_3 layer compounds exhibit susceptibility behavior reminiscent of antiferromagnetic materials. For example, $MnPSe_3$ susceptibility behavior was examined[3] in the 77–400 K range and its observed paramagnetic moment was readily explained by assuming the existence of a localized 2+ transition-metal ion. Other MPX_3 systems have been found to exhibit the same type of magnetic behavior as $FePSe_3$.[2,3] Perhaps the most conclusive evidence regarding whether the transition metal M in an MPX_3 system is divalent or not comes from the spectral features of low-energy optical absorption edge (0.1–3 eV) region of these materials. Brec *et al.*[4] have performed lower-energy optical absorption measurements on single crystals of $NiPS_3$, $FePS_3$, $FePS_3$, $MnPS_3$, $MnPSe_3$, and $CdPS_3$, and in all these materials, there has been observed rather intense d-d–"like" transitions (at photon energies close to the absorption edge), and these d-d–"like" transitions are reminiscent of those that are normally present on spectral features of Mn^{2+}, Fe^{2+}, and Ni^{2+} multiplets. The most convincing evidence of the existence of intense (low photon energy) $3d$-$3d$ transitions in these MPX_3 systems is provided by infrared- and visible- (0.5–3 eV) region optical absorption spectra of $MnPS_3$, $FePS_3$, and $NiPS_3$ obtained recently by Coić[5] (and co-workers) at the University of Nantes in France. The spectral features on the optical absorption spectrum of

$NiPS_3$ (Ref. 5) (especially) are characteristic of Ni^{2+} multiplets as observed in NiO.[15]

We also know (as already mentioned in earlier sections of this paper) from the magnetic moments determined in the paramagnetic region that the values of the magnetic moments of these materials are within the range expected for *high-spin divalent* metal ions in a nearly octahedral environment. Since these materials are so highly magnetic (implying spin pairing and spin alignment of $3d$ states), we deduce that the *high-spin divalent* metal (2+) ion $3d$ orbitals exist as localized (rather than band) states within the electronic bonding (in the $\sigma\sigma^*$ gap) of an MPX_3 system. Since (as mentioned in Sec. II), the Mn^{2+}, Fe^{2+}, and Ni^{2+} ions and P_2 pairs are octahedrally bonded to the X (chalcogen or ligand) atoms, we are therefore dealing with a manganese (II) or Fe (II) or Ni (II) complex in which the 2+ transition-metal ion finds itself in octahedral chalcogen surroundings. The octahedral ligand field will therefore split the (*high-spin* configuration) ground states of (i) (Mn^{2+}) d^5 orbitals into t_{2g}^3, e_g^2, (ii) (Fe^{2+}) d^6 orbitals into t_{2g}^4, e_g^2, and (iii) (Ni^{2+}) d^8 into t_{2g}^6, e_g^2. The t_{2g} (d_{xy}, d_{xz}, d_{yz}) states will be positioned nearer the valence band than the e_g states because the former states have electron densities which are concentrated close to the ligands, and therefore the t_{2g} states are more stable than the e_g states (see Figs. 10–12).

Figure 9 shows a block diagram of the states involved in the formation of a band model for an $M_2P_2S_6$ formula unit; the divalent transition metal (say Mn) contributes the $3d^54s^2$ states, phosphorus (P) contributes $3s^23p^3$ states. It has already been

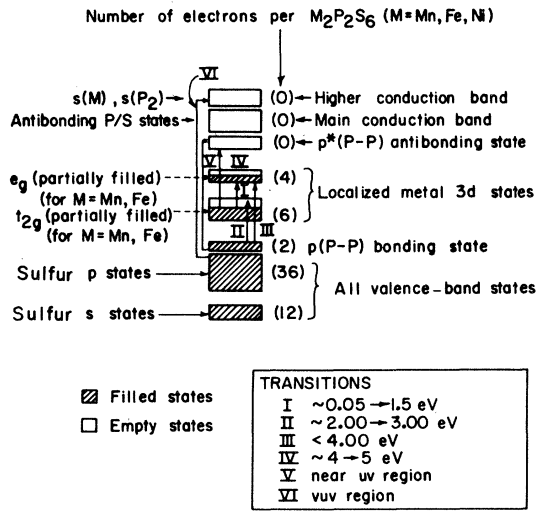

FIG. 9. Possible banding arrays for an MPX_3 layer material and general types of interband transitions that lead to the optical properties of these compounds.

mentioned that $FePS_3$ layer-type materials have a crystallographic structure which is related to that of cadmium chloride ($CdCl_2$) or TiS_2 with the iron (Fe^{2+}) ions and phosphorus-phosphorus pairs (P_2) occupying the cadmium or titanium positions. Therefore in $FePS_3$, we have, essentially, FeS_6 and P_2S_6 octahedral groups.

A simple electronic band model of an MPS_3 layer-structure compound that is consistent with (i) the electron states and the number of electrons available to fill these states and (ii) the experimental observation that these MPS_3 layer compounds exhibit magnetic behavior reminiscent of antiferromagnetic materials with discrete and localized $3d$ states can be obtained if we consider the *ionic extreme* of the Wilson-Yoffe[16] band model for layered dichalcogenides. In other words, our band model for an MPS_3 layer-type system will assume that there is little mixing of the sulfur (S) p with the metal (M) d states in the valence- or conduction-band states. Let us consider the doubled formula unit $M_2P_2S_6$ so that one P_2 pair [caused by the short (~2.2 Å) P–P bond distance—see Figs. 1 and 2] can be included in the counting of electrons available to fill the valence-band states. In this ionic band-model scheme with a divalent M^{2+} metal, the P_2 *pair has a formal valence* +8—that is, there is *one electron per* P used in the making of a P–P bond. This P–P bond will then produce two states, viz., one bonding P–P state (filled by *two* P electrons) with an energy in or near the predominantly S valence band and an antibonding P–P state (empty) with an energy that will be near but above the metal (M) e_g levels (see Figs. 9–12). Thus in our band model, the P_2^{8+} is behaving just like another metal in the Wilson-Yoffe band-model scheme. The valence band of an MPS_3 layer material will be largely based on the S p and s states, with the s band lying well below the p bands as shown in Fig. 9. In this *doubled* $M_2P_2S_6$ formula unit, there will be 48 valence-band states derived from each of the sulfur $3p$ ($6\times6=36$) and the sulfur $3s$ ($6\times2=12$) orbitals. The number of electrons available to fill the valence-band states is obtained as follows: $6\times6=36$ from S_6 (where each sulfur contributes $3s^23p^4$ electrons) *plus* $2\times2=4$ from the metal M_2 (where each metal contributes its $4s^2$ electrons) *plus* $2\times4=8$ from the P_2^{8+} [where each phosphorus (P) contributes $3s^23p^2$ electrons, *and not* $3s^23p^3$, because, as we mentioned above, one electron per P has already been used in the making of a P–P bond] for an overall total of 48 electrons. These 48 electrons will then fill the valence-band states of the doubled formula unit $M_2P_2S_6$ as indicated in Fig. 9. We must emphasize that since our band model for the MPS_3 layer systems considers the

ionic extreme of the Wilson-Yoffe band model, we have assumed little mixing of the sulfur (S) p and metal (M) d states in the valence or conduction bands. This neglect of covalent mixing between p (S) and d (M) states is *not a serious flaw* of our simple band model for an MPS_3, layer system, *at this level of discussion,* as one can readily estimate the extent and effect of the mixing from past experience with other chalcogenide first-principles band calculations. However, we are aware of the fact that this extreme ionic model is not very realistic for the S and P bonds since their ionicity difference is small and consequently, instead of the bonding states having all S character and antibonding states having all P character as is the case in the ionic model we have proposed, there would be considerable mixing of the orbitals on S and those on P in both the bonding and antibonding states, *but this would not change the counting* of *states*. We would like to further point out that while our ionic band model starts with a P_2^{8+} cation, the *real charge* on the P_2 pair will be quite small due to the above covalent mixing. Similar comments apply to the M–S bonds in the MPS_3 layer systems.

Using the electron states in Fig. 9 as a basis, we have proposed simple schematic electronic-band models for $MnPS_3$, $FePS_3$, and $NiPS_3$ as shown in Figs. 10, 11, and 12, respectively. Therefore, in our view, a simple band model for an MPS_3 layer system consists of a main p (S) valence band with a filled P–P bonding state lying just above the valence band (see Figs. 10–12). Because of the significant paramagnetic and antiferromagnetic behavior of these $FePS_3$ layer-type materials,[1-3] we envisage the transition-metal (M) $3d$ (e_g and t_{2g}) states as localized and discrete

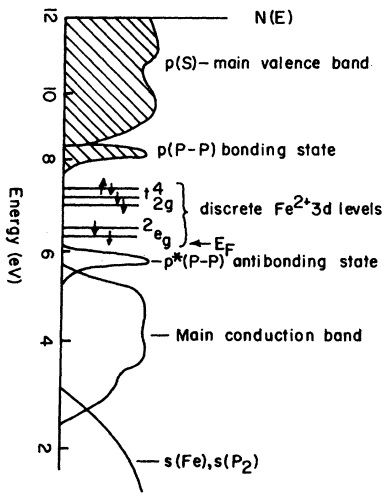

FIG. 11. Proposed band model for $Fe^{2+}PS_3^{2-}$.

levels (not bands) between the valence-band and conduction-band states. The empty antibonding P–P state lies just above the e_g state, i.e., nearer the main conduction which (for a nonionic model) will consist of a covalent admixture of antibonding P and S states. Higher conduction bands will consist of the empty $s(M)$ and $s(P_2)$ states. Since Mn^{2+}, Fe^{2+}, and Ni^{2+} cations all have unfilled $3d$ shells, it is reasonable to suggest that the Fermi level (E_F) in these MPS_3 layer systems probably lies within these localized and discrete $3d$ states.

C. Discussion

From our proposed band models of $MnPS_3$, $FePS_3$, and $NiPS_3$ (Figs. 10, 11, and 12, respectively), a qualitative study can explain why the high photon-energy reflectivity spectra of these three materials are bound to be so grossly simi-

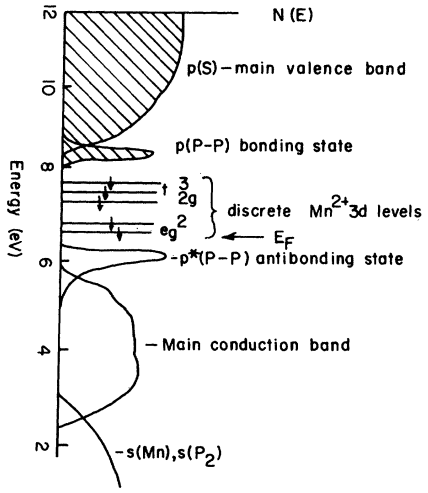

FIG. 10. Proposed band model for $Mn^{2+}PS_3^{2-}$.

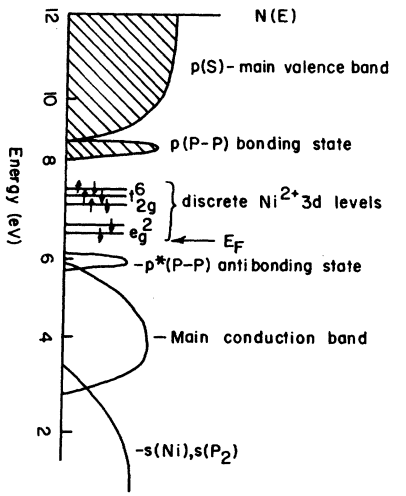

FIG. 12. Proposed band model for $Ni^{2+}PS_3^{2-}$.

lar. At photon energies close to or less than the band-gap energies of these materials (typically 1 → 3 eV),[4] we would first get (transition I in Fig. 9) weak $t_{2g} \rightarrow e_g$ (d-d) transitions[15,17] and then the p(S), p(P–P bonding) → $d(t_{2g}, e_g)$ transitions (transitions II and III in Fig. 9). All such transitions (from valence band to discrete $3d$ orbital levels) would lead to different reflectivity features because of the different ground-state-occupancy schemes for d orbitals in octahedral ligand fields. However, at the near- and far-ultraviolet regions (4 → 14 eV or more), all the three materials will exhibit grossly similar reflectivity spectra because of the similar strong p(S), p(P_2 pairs) bonding → nonbonding p^*(S) states and p^*(P_2 pairs antibonding states) transitions (V and VI in Fig. 9). Also the p(S) valence band → excited states (t^*_{2g}, e^*_g) of the d orbitals and the $(t_{2g}, e_g) \rightarrow p^*$ (P_2 antibonding), p^*(S) transitions would all be identical in the three materials, again leading to similarities in the three reflectivity spectra.

Other physical considerations which explain the gross similarities of the vuv reflectivity spectra of these Mn II PS_3 complex systems are the following: (a) the metal–metal (given by "a" lattice constant of each crystal) distance (in Å within layers of each compound, (b) the size of the 2+ ionic radii (in Å) of Mn^{2+}, Fe^{2+}, and Ni^{2+}, and (c) the electronegativities of Mn, Fe, and Ni. The values of these constants are shown in Table II.

The "a" values are quoted from Taylor *et al.*[1]; the $r_{M^{2+}}$ (ionic radius) and electronegativity values are quoted from Pauling.[18] From Table II, we note that $MnPS_3$ and $FePS_3$ have almost equal; moreover, the electronegativity values for Mn^{2+} and Fe^{2+} are almost equal too. All these factors imply that metal-metal overlaps and ligand-field effects in $MnPS_3$ and $FePS_3$ would be equivalent resulting in roughly equivalent d (localized) levels and s-band separations, widths, and overlaps. This further explains the close similarities in the vuv spectra of $MnPS_3$ and $FePS_3$ compounds. The similarities in reflectivity features of $MnPS_3$ and $FePS_3$ can be further inferred from the proposed band models in Figs. 10 and 11. In these band models, we note that the only difference between the two models is just one electron (with spin down) on the (Fe^{2+}) t_{2g} ground state. Therefore we would expect p(S), p(P–P bonding) → t_{2g} and p(S); p(P–P bonding) → e_g transitions to be equivalent in $MnPS_3$ and $FePS_3$. Also from the above-mentioned arguments on the relative values of the "a" lattice constants, ionic radii, and electronegativities for Mn^{2+} and Fe^{2+}, we would also expect p(S), p(P–P bonding) → s (Mn), p^*(P–P antibonding), and nonbonding p^*(S) transitions to be comparable, thus leading to similarities in the vuv spectra of both compounds ($MnPS_3$ and $FePS_3$).

TABLE II. The "a", $r_{M^{2+}}$, and electronegativity values for $MnPS_3$, $FePS_3$, and $NiPS_3$.

Compound	a (Å)	$r_{M^{2+}}$	Electronegativity
$MnPS_3$	6.088	0.80	1.60
$FePS_3$	5.970	0.76	1.64
$NiPS_3$	5.808	0.68	1.91

On the other hand, the vuv spectrum of $NiPS_3$ appears to have some dissimilarities to those of $MnPS_3$ and $FePS_3$. The explanation for these differences lies in the values of the parameters on Table II and the unique ground-state-occupancy scheme for d orbitals in an octahedral complex with d^8 (Ni^{2+}) configuration. From Table II, we note that the Ni^{2+} has the smallest "a" lattice constant and the smallest 2+ ionic radius of the three cations (Mn^{2+}, Fe^{2+}, Ni^{2+}) but has the largest electronegativity value. The smaller "a" lattice constant for $NiPS_3$ and the smaller ionic radius (0.68 Å) of Ni^{2+} both imply that there is considerable Ni–Ni overlap in $NiPS_3$ and this leads to broader metal-orbital-based conduction bands in $NiPS_3$ than in $MnPS_3$ or $FePS_3$. These differences inevitably lead to differences in the spectra of $NiPS_3$ and Mn or Fe compounds.

We have already mentioned, earlier on, that there appears to be much more pronounced reflectivity structure (between 4 and 7 eV) on $MnPS_3$ and $FePS_3$ than on the $NiPS_3$ spectrum. The reason for this difference becomes clear if we study the d-orbital occupancies in Figs. 10–12. Because of the unique d^8-orbital configuration, the ground state t_{2g} is completely full for Ni^{2+} and yet half-full for Mn^{2+} (d^5) and two-thirds full for Fe^{2+} (d^6) Therefore, this means that at low photon energies (infrared, visible, and near-uv) there will be no p(S), p(P–P) → t_{2g}(Ni^{2+}) transitions in $NiPS_3$ and yet such transitions will occur in $MnPS_3$ and $FePS_3$. This probably explains why there are differences in the vuv reflectivity features between $NiPS_3$ and $MnPS_3$ or $FePS_3$ spectra at low photon energies.

Overall, there appears to be less fine structure on the $NiPS_3$ spectrum than on the $MnPS_3$ and $FePS_3$ spectra. Again the cause for this difference lies in the differences between metal–metal distances and hence metal-metal overlaps between Ni^{2+} and Mn^{2+} or Fe^{2+} chalcogenophosphates. As we noted earlier, the smaller ionic radius (0.68 Å) of Ni^{2+} and the smaller "a" lattice constant for $NiPS_3$ both imply that there is more Ni–Ni overlap in the $NiPS_3$ band structure (this leads to broader metal-orbital-based conduction bands in $NiPS_3$) than in the other two compounds. Broader bands of $NiPS_3$ will overlap more and this leads to less

gaps between such bands. An interband transition is more likely to occur between two separate nonoverlapping bands than between two strongly overlapping broader bands.

We mentioned earlier that if the three spectra are superposed, the sharp peak at ~7 eV on the $NiPS_3$ spectrum has a shift of ~0.3 eV to low energies relative to similar peaks on $MnPS_3$ and $FePS_3$ spectra and that the peak at ~10 eV on the $NiPS_3$ has a shift of ~0.5 eV to higher energies relative to corresponding peaks on the $MnPS_3$ and $FePS_3$ spectra. These observations further underline the broad similarities between $NiPS_3$ and $MnPS_3$ or $FePS_3$ spectra already discussed. These shifts in the peaks of the $NiPS_3$ spectrum probably imply that the widths of the valence bands in $NiPS_3$ are different from the corresponding valence-band width in $MnPS_3$ or $FePS_3$. Photoemission (XPS) measurements would determine the exact valence-band widths in these materials. These XPS measurements are currently under plan at Ames Laboratory of Iowa State University, Ames, Iowa. We hope to publish such measurements in our next paper on these MPS_3 systems.

In our discussion so far, no mention has been made of the possibility of the interband transition of the type $d(t_{2g}, e_g) \rightarrow s(M), p^*(P_2)$ antibonding states), $p^*(S)$, and $p(S), p(P_2$ bonding$) \rightarrow$ localized excited states t_{2g}^* and e_g^*. Such transitions are possible (and probably occur) but in view of the sharp and strong reflectivity features in the 4–14 eV range observed in these materials, one is strongly tempted to speculate that, overall, $p(S) \rightarrow s(M)$ transitions (where X and M have the same meanings as before) are the dominant transitions due to their possible larger oscillator strengths than, say, $p(X) \rightarrow d(M)$ or $d(M) \rightarrow s(M)$ transitions. These latter transitions are most probably weak and therefore will not show on a reflectivity spectrum.

V. CONCLUSION

The reasons for the similarities of the vuv reflectivity spectra of these $FePS_3$-type layer compounds were discussed, in detail, in the above paragraphs and we can summarize the arguments as follows: Consider two such materials represented by the chemical formulas MPS_3 and $M'PS_3$, where M' and M are first-row-series transition metals, and both metals have a divalent ionic valency (and equivalent 2+ ionic radii) and their d orbitals are subjected to the same type (octahedral or tetrahedral) of ligand field, (such that ligand-field splittings of the d orbitals are similar); then these materials would be expected to exhibit high-energy optical transitions because at such high proton energies, the discrete and localized d states (observable in the absorption-edge region) do not contribute to the transitions. In other words, the transition metals (from which these d orbitals come), at high photon energies, do not contribute significantly to the interband transitions. The main contributor to high-energy interband transitions in $FePS_3$-type compounds is the P_2S_6 complex which is present in all MPX_3 compounds. As already mentioned in the main discussion, the valence band of these compounds consists mainly of $p(S)$ and $p(P_2$ pairs) bonding states and the conduction band consists of an admixture of $p^*(P_2$ pairs) antibonding and the $p^*(S)$ states. So at high photon energies, we are mainly observing an $FePS_3$-type material reflectivity spectrum which is due to $p(S) \rightarrow p^*(P_2$ pairs) and $p^*(S)$ transitions which are the same for all MPX_3 systems irrespective of the metal and the occupancy of its localized d states. The $p(S) \rightarrow d(M)$ transitions (where $M = Mn, Fe, Ni$) will occur at photon energies less than 4 eV. The presence of the localized $3d$ states in the vicinity of the Fermi energy is manifest at very low photon energies.[3-5] In view of these arguments, we would like to suggest that the electronic band structures of MPX_3 compounds are similar. These MPX_3 systems, like the ZrS_3-structured compounds[14] we reported in another paper, are a challenge to band theorists who, using modern and sophisticated computing methods, may be able to obtain meaningful band structures of solids of this complexity. The striking similarities of the reflectivity spectra of $MnPS_3$, $FePS_3$, and $NiPS_3$ must also be a result of the structural isomorphy of these materials.

ACKNOWLEDGMENTS

The Ames Laboratory is operated for the U.S. Department of Energy by Iowa State University under Contract No. W-7405-Eng-82. This research was supported by the Director for Energy Research, Office of Basic Energy Sciences, WPAS-AK-01-02. One of us, F. S. K., would like to thank the Association of Commonwealth Universities, London, for the award of the Commonwealth fellowship to do research at the Cavendish Laboratory, University of Cambridge, England, and Trinity College, Cambridge, for the award of a Research Studentship. We are also deeply grateful to Miss Lawrence Coic (Université Nantes, France) for kindly lending us her large and beautiful single crystals of $MnPS_3$, $FePS_3$, and $NiPS_3$. We would like to thank Dr. A. R. Beal, Dr. D. W. Bullett, and Dr. A. D. Yoffe for numerous illuminating discussions.

*Present Address: Ames Laboratory, Department of Energy, Iowa State University, Ames, Iowa 50011, and Department of Physics, Iowa State University, Ames, Iowa 50011.

[1]B. E. Taylor, J. Steger, and A. J. Wold, J. Solid State Chem 7, 461 (1973).
[2]B. E. Taylor, J. Steger, A. J. Wold, and E. Kostiner, Inorg. Chem. 13, 2719 (1974).
[3]C. Berthier, Y. Chabe, and M. Minier, Solid State Comm. 28, 327 (1978).
[4]R. Brec, D. Schleich, G. Ouvrard, A. Luisy, and J. Rouxel, Inorg. Chem. 18, 1814 (1979).
[5]Lawrénce Coić (private communication).
[6]A. H. Thompson and M. S. Whittingham, Mater. Res. Bull. 12, 741 (1977).
[7]M. S. Whittingham, Science 192, 1126 (1976).
[8]S. Yamanaka, H. Kabayashi, and M. Tanaka, Chem. Lett. Jpn. 4, 329 (1976).
[9]F. Kanamaru, S. Otani, and M. Koizumi, in Extended Abstracts of the Fifth International Conference on Solid Composition of Transition Elements, Uppsala, Sweden, 1976 (unpublished), p. 36.
[10]W. Klingen, G. Eulenberger, and H. Hahn, Naturwissenschaften 55, 229 (1968).
[11]W. Klingen, G. Eulenberger, and H. Hahn, Meeting on Transition Metal Compounds, Oslo, Norway, 1969 (unpublished).
[12]W. Klingen, G. Eulenberger, and H. Hahn, Naturwissenschaften 57, (2) 88 (1970).
[13]R. Nitsche and P. Wild, Mater. Res. Bull. 5, 419 (1971).
[14]F. S. Khumalo and H. P. Hughes, Phys. Rev. B 22, 2078 (1980).
[15]D. Adler and J. Feinleib, Phys. Rev. B 2, 3112 (1970).
[16]J. A. Wilson and A. D. Yoffe, Adv. Phys. 18, 193 (1969).
[17]S. Sugano, Y. Tanabe, and H. Kamimura, *Multiplets of Transition-Metal Ions in Crystals* (Academic, New York, 1970).
[18]Linus Pauling, *The Nature of the Chemical Bond*, 3rd ed. (Cornell University Press, Ithaca, 1960).